Study of the decays $\chi_{cJ} \to \Lambda\bar{\Lambda}\phi$

M. Ablikim *et al.*[*]
(BESIII Collaboration)

(Received 2 June 2024; accepted 23 July 2024; published 15 August 2024)

Based on $(2712.4 \pm 14.3) \times 10^6$ $e^+e^- \to \psi(3686)$ events collected with the BESIII detector operating at the BEPCII Collider, we report the first evidence of $\chi_{c0} \to \Lambda\bar{\Lambda}\phi$ decays and the first observation of $\chi_{c1,2} \to \Lambda\bar{\Lambda}\phi$ decays, with significances of 4.1σ, 11.3σ and 13.0σ, respectively. The decay branching fractions of $\chi_{c0,1,2} \to \Lambda\bar{\Lambda}\phi$ are measured to be $(2.99 \pm 1.24 \pm 0.19) \times 10^{-5}$, $(6.01 \pm 0.90 \pm 0.40) \times 10^{-5}$, and $(7.13 \pm 0.81 \pm 0.36) \times 10^{-5}$, where the first uncertainties are statistical and the second systematic. No obvious enhancement near the $\Lambda\bar{\Lambda}$ production threshold or excited Λ state is found in the $\Lambda\phi$ (or $\bar{\Lambda}\phi$) system.

DOI: 10.1103/PhysRevD.110.032016

I. INTRODUCTION

In the quark model, the $\chi_{cJ}(J = 0, 1, 2)$ mesons are identified as ^3P_J charmonium states. Due to the conservation of parity, it was long considered impossible for e^+e^- annihilation to directly produce them. As a result, the decays of χ_{cJ} have not been studied as extensively as the vector charmonium states J/ψ and $\psi(3686)$ in both experiment and theory. However, χ_{cJ} mesons can be produced via radiative decays of the $\psi(3686)$ with a sizable branching fraction (BF) of about 9% [1] for each χ_{cJ} state, thereby offering an ideal environment to investigate their properties and decays.

Studies of the processes involving the $B\bar{B}V$ final states, where B and V denote baryons and vector mesons, respectively, are valuable in the search for possible $B\bar{B}$ threshold enhancements and excited baryon states decaying into BV. A threshold enhancement in the $p\bar{p}$ system was first observed in the $J/\psi \to \gamma p\bar{p}$ decay at BESII [2] and was later confirmed by BESIII with improved precision [3]. Subsequently, an enhancement around the $\Lambda\bar{\Lambda}$ production threshold was observed in various processes, such as $e^+e^- \to \phi\Lambda\bar{\Lambda}$ [4], which disfavored an interpretation of the enhancement as originating from the $\eta(2225) \to \Lambda\bar{\Lambda}$ decay [5]. In addition, the excited state $\Lambda(1670)$ was observed in the near-threshold reaction $K^-p \to \Lambda\eta$ [6] and in the $\Lambda\eta$ mass spectra in the charmonium decay of $\psi(3686) \to \Lambda\bar{\Lambda}\eta$ [7]. However, experimental results on the $\Lambda\bar{\Lambda}$ production threshold enhancement and on excited Λ states decaying into $\Lambda\phi$ are still limited. Comprehensive investigations of the $B\bar{B}V$ system in a wide range of charmonium decays are desirable. So far, only a few studies of P wave charmonium decays, $\chi_{cJ} \to B\bar{B}V$, have been performed [1,8–10]. A search for similar decay modes may provide an opportunity to further investigate the potential enhancement at the $\Lambda\bar{\Lambda}$ production threshold and the nature of excited Λ states.

In this paper, by analyzing $(2712.4 \pm 14.3) \times 10^6$ $\psi(3686)$ events [11] collected with the BESIII detector, we present the first experimental studies of $\chi_{cJ} \to \Lambda\bar{\Lambda}\phi$ decays.

II. BESIII DETECTOR AND MONTE CARLO SIMULATION

The BESIII detector [12] records e^+e^- collisions provided by the BEPCII storage ring [13]. The cylindrical core of the BESIII detector covers 93% of the full solid angle and consists of a helium-based multilayer drift chamber (MDC), a plastic scintillator time-of-flight system (TOF), and a CsI(Tl) electromagnetic calorimeter (EMC), which are all enclosed in a superconducting solenoidal magnet providing a 1.0 T magnetic field. The magnet is supported by an octagonal flux-return yoke with modules of resistive plate muon counters interleaved with steel. The charged-particle momentum resolution at 1 GeV/c is 0.5%, and the dE/dx resolution is 6% for the electrons from Bhabha scattering at 1 GeV. The EMC measures photon energy with a resolution of 2.5% (5%) at 1 GeV in the barrel (end-cap) region. The time resolution of the TOF barrel part is 68 ps, while that of the end-cap part is 110 ps. The end cap TOF system was upgraded in 2015 using multigap resistive plate chamber technology, providing a time resolution of

[*]Full author list given at the end of the article.

Published by the American Physical Society under the terms of the Creative Commons Attribution 4.0 International license. Further distribution of this work must maintain attribution to the author(s) and the published article's title, journal citation, and DOI. Funded by SCOAP³.

60 ps, which benefits 86% of the data used in this analysis [14–16].

Monte Carlo (MC) simulated data samples are produced with a GEANT4-based [17] software package, which includes the geometric description [18] of the BESIII detector and the detector response. They are used to optimize the event selection criteria, and estimate the signal efficiency and the level of background. The simulation models the beam-energy spread and initial-state radiation in the e^+e^- annihilation using the generator KKMC [19,20]. The inclusive MC sample includes the production of the $\psi(3686)$ resonance, the initial-state radiation production of the J/ψ meson, and the continuum processes incorporated in KKMC. Particle decays are generated by EvtGen [21,22] for the known decay modes with BFs taken from the Particle Data Group (PDG) [1] and LUNDCHARM [23,24] for the unknown ones. Radiation from charged final-state particles is included using the PHOTOS package [25].

To determine the detection efficiency for each signal process, signal MC samples are generated with a modified data-driven generator BODY3 [21,22], which simulates contributions from different intermediate states in data for a given three-body final state, as discussed in Sec. IV.

III. EVENT SELECTION

The $\Lambda/\bar{\Lambda}$ and ϕ particles are reconstructed via their decays $\Lambda/\bar{\Lambda} \to p\pi^-/\bar{p}\pi^+$ and $\phi \to K^+K^-$. Charged tracks detected in the MDC are required to be within a polar angle θ such that $|\cos\theta| < 0.93$, where θ is defined with respect to the symmetry axis of the MDC. The Λ and $\bar{\Lambda}$ candidates are reconstructed by combining pairs of oppositely charged tracks with pion and proton mass hypotheses satisfying a secondary vertex constraint [26]. Events with at least one $p\pi^-(\Lambda)$ and one $\bar{p}\pi^+(\bar{\Lambda})$ candidate are selected. In the case of multiple $\Lambda\bar{\Lambda}$ pair candidates, the one with the minimum value of $\sqrt{(M_{p\pi^-} - m_\Lambda)^2 + (M_{\bar{p}\pi^+} - m_{\bar{\Lambda}})^2}$ is chosen, where $M_{p\pi^-}$ ($M_{\bar{p}\pi^+}$) is the invariant mass of the $p\pi^-$ ($\bar{p}\pi^+$) system, and m_Λ ($m_{\bar{\Lambda}}$) is the know mass of $\Lambda(\bar{\Lambda})$ [1]. Considering that $\Lambda(\bar{\Lambda})$ has a relatively long lifetime, we require the decay length of $\Lambda(\bar{\Lambda})$ to be greater than zero. The charged tracks other than those originating from the $\Lambda\bar{\Lambda}$ pair are taken as originating from the ϕ decay. For these tracks, the distance of closest approach to the e^+e^- interaction point must be less than 10 cm in the beam axis and less than 1 cm in the plane perpendicular to this axis. The measurements of the flight time in the TOF and $\mathrm{d}E/\mathrm{d}x$ in the MDC for each charged track are combined to compute particle identification (PID) confidence levels for the pion, kaon, and proton hypotheses. Tracks are identified as K if the confidence level for the kaon hypothesis is the highest among the three hypotheses of π, K, and p. The ϕ signal is reconstructed by the invariant mass of the charged kaon pair's candidate with $|M_{K^+K^-} - m_\phi| < 18$ MeV$/c^2$, and the region of $1055 < M_{K^+K^-} < 1127$ MeV$/c^2$ is taken as the ϕ sideband, where m_ϕ is the ϕ known mass [1]. The range here is determined based on the mass resolution obtained from the signal MC sample.

Photon candidates are identified using showers in the EMC. The deposited energy of each shower must be greater than 25 MeV in the barrel region ($|\cos\theta| < 0.80$) or greater than 50 MeV in the end-cap region ($0.86 < |\cos\theta| < 0.92$). To suppress electronic noise and energy depositions not associated with the event, the EMC cluster timing from the reconstructed event start time is further required to satisfy $0 \le t \le 700$ ns.

To further suppress the combinatorial background, a four-constraint (4C) kinematic fit imposing four-momentum conservation under the hypothesis of $\psi(3686) \to \gamma\Lambda\bar{\Lambda}K^+K^-$ is performed. The combination with the minimum χ^2_{4C} is retained for further analysis if the number of photons is more than one. Furthermore, the χ^2_{4C} of the kinematic fit is required to be less than 60 by optimizing the figure of merit $\frac{\varepsilon}{\frac{a}{2}+\sqrt{N_{bkg}}}$ [27] via the χ_{c2} decay mode, where ε is the detection efficiency, $a = 3$ is the expected significance of this measurement process, and N_{bkg} is the number of background events estimated from the inclusive $\psi(3686)$ MC sample. Additionally, the background events of $\chi_{cJ} \to \Omega^-\bar{\Omega}^+$ are vetoed by the two-dimensional (2D) mass window, $|M_{\Lambda K^-} - m_{\Omega^-}| > 12$ MeV$/c^2 \cup |M_{\bar{\Lambda}K^+} - m_{\bar{\Omega}^+}| > 12$ MeV$/c^2$, where $m_{\Omega^-(\bar{\Omega}^+)}$ is the known mass of the $\Omega^-(\bar{\Omega}^+)$ baryon [1].

Figure 1 shows the 2D distribution of the invariant mass for $p\pi^-$ versus $\bar{p}\pi^+$ for data after all selection criteria are applied. A clear $\Lambda\bar{\Lambda}$ pair signal can be observed. The one-dimensional (1D) Λ and $\bar{\Lambda}$ signal region are defined as $|M_{p\pi^-(\bar{p}\pi^+)} - m_{\Lambda(\bar{\Lambda})}| < 6$ MeV$/c^2$. The 2D signal region of $\Lambda\bar{\Lambda}$ and its 2D $\Lambda\bar{\Lambda}$ sideband regions are shown in Fig. 1.

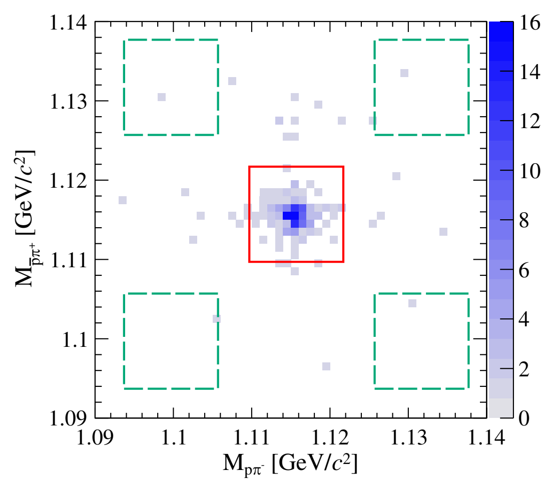

FIG. 1. The 2D distribution of $M_{\bar{p}\pi^+}$ versus $M_{p\pi^-}$ of the accepted candidates, where the box in red solid lines is the $\Lambda\bar{\Lambda}$ signal region, and the boxes in green dashed lines are the sideband regions.

Potential remaining background contributions are investigated with the inclusive $\psi(3686)$ MC events, using the event-type analysis tool TopoAna [28]. The dominant background comes from the nonresonant $\psi(3686)$ decay of $\psi(3686) \to \gamma\Lambda\bar{\Lambda}\phi$.

To investigate possible continuum background, the same selection criteria are applied to the data samples collected at the center-of-mass energies of 3.650 GeV and 3.682 GeV, corresponding to an integrated luminosity of 454 pb^{-1} and 404 pb^{-1}. No event survives after applying all the selection criteria. Hence, the continuum background is considered to be negligible.

IV. SIGNAL YIELDS

The signal yields of the $\chi_{c0,1,2} \to \Lambda\bar{\Lambda}\phi$ decays are obtained by performing a simultaneous fit to the $M_{\Lambda\bar{\Lambda}K^+K^-}$ spectra of the events in the ϕ signal and sideband regions. In the fit, the signal shapes are described by the MC-simulated shapes convolved with a Gaussian function, and their parameters are floated and shared by all χ_{cJ} signal contributions.

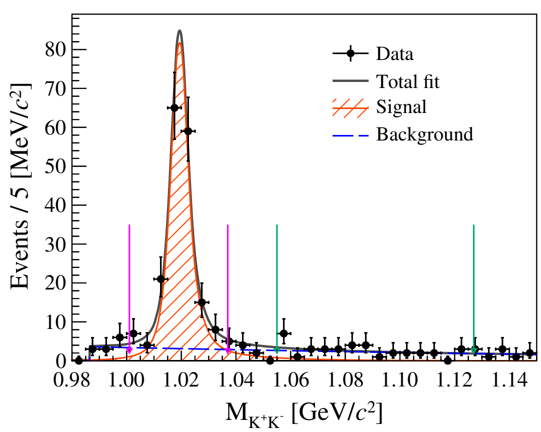

FIG. 2. Fit to the $M_{K^+K^-}$ distribution of the accepted candidates. The pink arrows show the ϕ signal region, and the pair of green arrows shows the ϕ sideband region.

We also examine the impact of fake Λ and $\bar{\Lambda}$ candidates. After considering the number of candidates in the 2D sideband region (denoted as four green boxes in Fig. 1) this background is judged to be negligible. The non-χ_{cJ} radiative background is described by the MC-simulated shape of the $\psi(3686) \to \gamma\Lambda\bar{\Lambda}\phi$ decay, and the number of events is taken as a free parameter. There is the possibility of a K^+K^- background that does not come from ϕ resonance. The shape of this background contribution is derived from the MC sample of $\psi(3686) \to \gamma\chi_{cJ}, \chi_{cJ} \to \Lambda\bar{\Lambda}K^+K^-$, and its yield is treated as a shared parameter for the two modes, with its contribution multiplied by a normalization factor f_ϕ. The normalization factors, f_ϕ, between the ϕ signal and sideband regions are determined to be 0.71 by comparing the numbers of background events in the ϕ signal and sideband regions, as shown in Fig. 2. Specifically, in the fitting of the K^+K^- invariant-mass spectrum, the signal component is modeled with the MC-simulated shape convolved with a Gaussian function to account for the possible difference in the mass resolution between data and MC simulation. The remaining combinatorial background shape is described by a reverse ARGUS function [29]. The fit result is shown in Fig. 3, and the obtained signal yields are summarized in Table I.

The significances of $\chi_{c1} \to \Lambda\bar{\Lambda}\phi$ and $\chi_{c2} \to \Lambda\bar{\Lambda}\phi$ are determined to be 11.3σ and 13.0σ, respectively, by comparing the difference of likelihoods with and without including each signal in the fit. To estimate the significance of $\chi_{c0} \to \Lambda\bar{\Lambda}\phi$, we apply another approach due to the low signal yield. We assume that the number of signal and background events in the χ_{c0} signal region follow a Poisson distribution with mean $n = s + b$ [30], where the signal region is $[m_{\chi_{c0}} - 22, m_{\chi_{c0}} + 22]$ MeV/c^2 (two times the mass resolution), with $m_{\chi_{c0}}$ the known χ_{c0} mass [1].

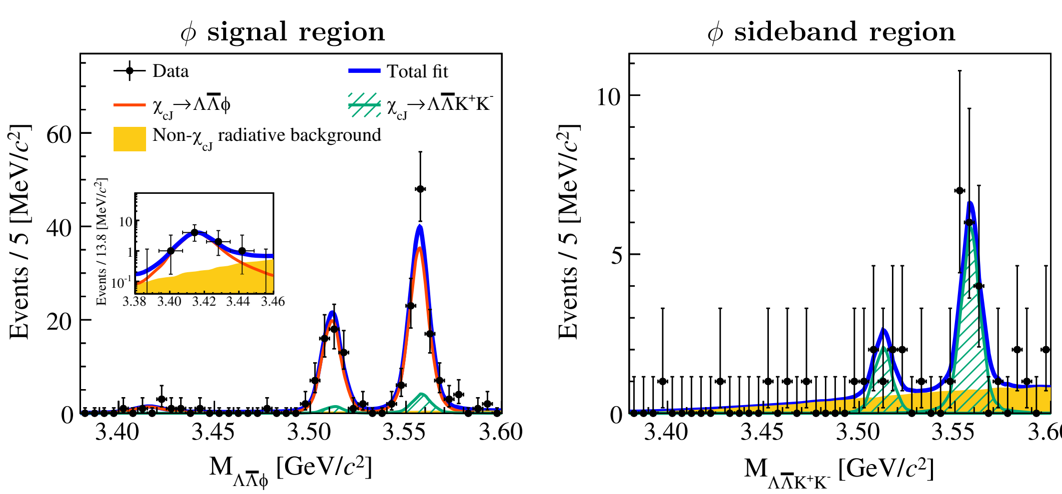

FIG. 3. Simultaneous fit to the $M_{\Lambda\bar{\Lambda}K^+K^-}$ distributions in the ϕ (left) signal and (right) sideband regions.

TABLE I. The signal yields ($N_{\rm obs}^{\chi_{cJ}}$), significances, efficiencies, and the obtained BFs. The first uncertainties are statistical and the second systematic. The significances include systematic uncertainties.

	χ_{c0}	χ_{c1}	χ_{c2}
$N_{\rm obs}^{\chi_{cJ}}$	7.2 ± 3.0	51.6 ± 7.7	94.4 ± 10.7
Significance (σ)	4.1	11.3	13.0
$\varepsilon(\chi_{cJ} \to \Lambda\bar{\Lambda}\phi)$ (%)	0.45	1.61	2.54
$\mathcal{B}(\psi(3686) \to \gamma\chi_{cJ}) \cdot \mathcal{B}(\chi_{cJ} \to \Lambda\bar{\Lambda}\phi)(\times 10^{-6})$	$2.92 \pm 1.22 \pm 0.19$	$5.86 \pm 0.87 \pm 0.39$	$6.79 \pm 0.77 \pm 0.35$
$\mathcal{B}(\chi_{cJ} \to \Lambda\bar{\Lambda}\phi)(\times 10^{-5})$	$2.99 \pm 1.24 \pm 0.19$	$6.01 \pm 0.90 \pm 0.40$	$7.13 \pm 0.81 \pm 0.36$

Here, $s = 6$ represents the expected number of signal events, while $b = 0.6$ represents the expected number of Poisson-distributed background events. All numbers are counted in the signal region where significant accumulations of events are expected to appear. Then the p value for the null hypothesis without a resonance (H_0) is

$$p(n_{\rm obs}) = P(n > n_{\rm obs}|H_0) = \sum_{n=n_{\rm obs}}^{\infty} \frac{b^n}{n!} e^{-b}$$
$$= 1 - \sum_{n=0}^{n_{\rm obs}-1} \frac{b^n}{n!} e^{-b},$$

where $n_{\rm obs}$ is the number of events observed in the signal region. The p value is obtained by calculating the probability of the number of background events fluctuating to the number of observed events in the χ_{c0} signal region. The p value for the $\chi_{c0} \to \Lambda\bar{\Lambda}\phi$ decay is 3.89×10^{-5}, corresponding to a significance of 4.1σ. In determining this significance, the systematic uncertainties are accounted for by repeating the fits with variations of the signal shape, background shape, and fit range.

The existence of potential intermediate states in the $\Lambda\bar{\Lambda}\phi$ final state are investigated through scrutiny of the Dalitz plots, except for the χ_{c0} mode, where the signal yield is too low. Figure 4 shows the invariant masses of different two-body combinations for $\chi_{c1,2}$ signals, after subtracting the background contributions using the normalized sideband events. No obvious structures are observed. Nevertheless, the mass spectra do not agree well with the signal MC shapes generated with the PHSP model, which will lead to a bias in the efficiency correction made based on this model. Therefore, the PHSP model is replaced by the modified data-driven generator BODY3 [21,22], which was developed to simulate different intermediate states in data for a given three-body final state. The Dalitz plot of $M^2_{\Lambda\phi}$ versus $M^2_{\bar{\Lambda}\phi}$ found in the data, including a binwise correction for backgrounds and efficiencies, is taken as an input to the

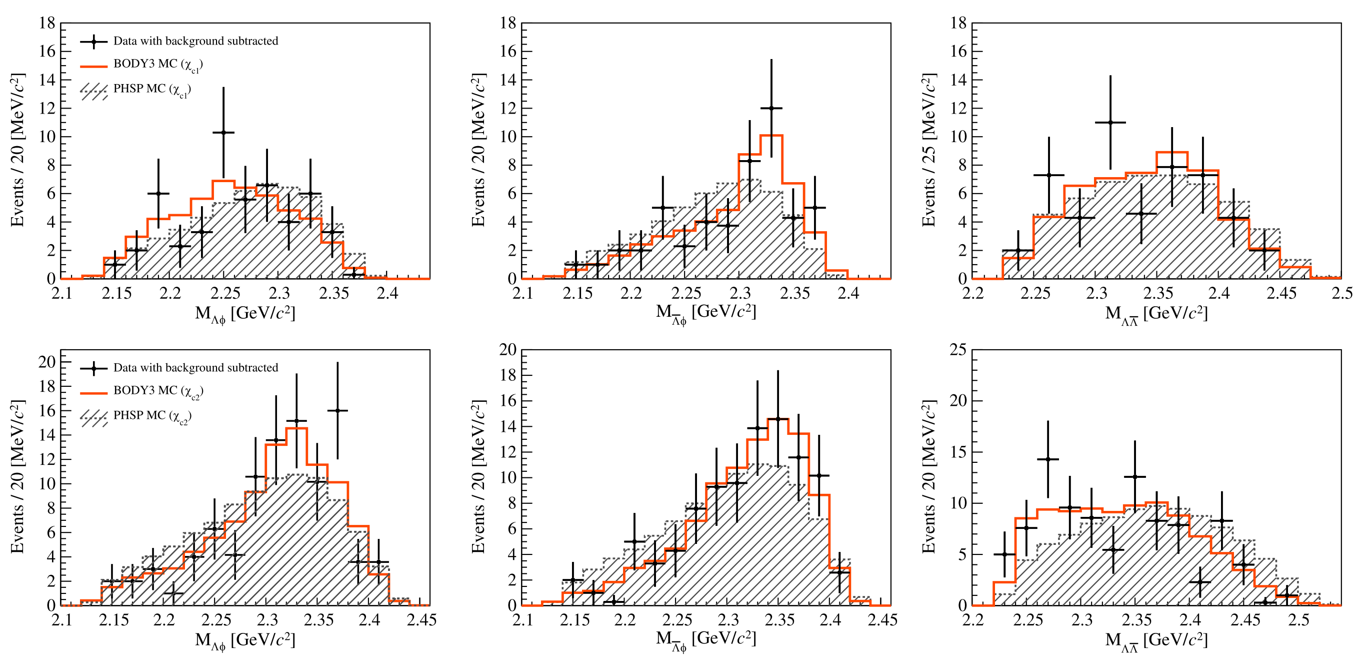

FIG. 4. Invariant-mass distributions of different two-body combinations of the decays of (top row) $\chi_{c1} \to \Lambda\bar{\Lambda}\phi$ and (bottom row) $\chi_{c2} \to \Lambda\bar{\Lambda}\phi$. The data are background subtracted. Two MC predictions are shown, one based on the PHSP model, the other on the BODY3 model.

BODY3 generator. The updated data-MC comparisons based on the BODY3 signal MC samples are shown in Fig. 4, where the data-MC agreement is improved compared to the PHSP model.

V. NUMERICAL RESULTS

The BFs of $\chi_{cJ} \to \Lambda\bar{\Lambda}\phi$ are calculated by

$$\mathcal{B}(\chi_{cJ} \to \Lambda\bar{\Lambda}\phi) = \frac{N_{\rm obs}^{\chi_{cJ}}}{N_{\psi(3686)}\prod_i \mathcal{B}_i \cdot \varepsilon(\chi_{cJ} \to \Lambda\bar{\Lambda}\phi)}, \quad (1)$$

where $N_{\rm obs}^{\chi_{cJ}}$ is the χ_{cJ} signal yield; $\prod_i \mathcal{B}_i$ is the product BFs of $\psi(3686) \to \gamma\chi_{cJ}$, $\Lambda \to p\pi$, and $\phi \to K^+K^-$, as taken from the PDG [1]; $N_{\psi(3686)}$ is the total number of $\psi(3686)$ events [11]; and $\varepsilon(\chi_{cJ} \to \Lambda\bar{\Lambda}\phi)$ is the detection efficiency. The measured BFs of each decay mode are summarized in Table I.

VI. SYSTEMATIC UNCERTAINTIES

Several sources of systematic uncertainty have been considered and are detailed below.

(1) *Kaon tracking*: The systematic uncertainty associated with the tracking efficiency is estimated with a control sample of $J/\psi \to K_S^0 K^\pm \pi^\mp$ decays, and determined to be 1.0% [31] for each kaon.

(2) *Kaon PID*: The systematic uncertainty associated with the kaon-PID efficiency is determined to be 1% [31] for each kaon, based on the same sample used to estimate the kaon tracking efficiency.

(3) *Photon reconstruction*: The systematic uncertainty arising from the knowledge of the photon reconstruction efficiency is assigned to be 1.0% [32], from studies of the control sample of $J/\psi \to \pi^+\pi^-\pi^0$ decays.

(4) *4C kinematic fit*: To assign the systematic uncertainty related to the 4C kinematic fit, control samples of $\psi(3686) \to \pi^+\pi^- J/\psi, J/\psi \to \Lambda\bar{\Lambda}$ and $\psi(3686) \to \eta J/\psi, J/\psi \to \Lambda\bar{\Lambda}\pi^+\pi^-$, events which have similar topologies as the signal modes are employed. The efficiency of the 4C kinematic fit is defined as the ratio of the signal yields with and without the same χ^2 requirement as the signal channel. The larger difference in efficiencies between data and MC simulation of the two control samples, 1.3%, is taken as the systematic uncertainty.

(5) $\Lambda(\bar{\Lambda})$ *reconstruction*: The combined efficiency including proton/antiproton and charged pion tracking, and Λ and $\bar{\Lambda}$ reconstruction are studied with a control sample of $J/\psi \to pK^-\bar{\Sigma}^0(\to\gamma\bar{\Lambda}) + \text{c.c.}$ decays. The differences in reconstruction efficiencies between data and MC simulation, 1.8% per Λ and 1.5% per $\bar{\Lambda}$, are taken as the corresponding systematic uncertainties.

(6) *Signal yield determination*

(a) *Mass window*: The systematic uncertainties associated with each mass window are estimated by varying each mass window by 1 standard deviation of the corresponding mass resolution. The larger change of the remeasured BF is taken as the corresponding systematic uncertainty.

(b) *Fit range*: To examine potential systematic uncertainty associated with the choice of fit range, we perform a Barlow test [33] to examine the significance of deviation (ζ) between the baseline fit and the systematic test, defined as

$$\zeta = \frac{|V_{\rm nominal} - V_{\rm test}|}{\sqrt{|\sigma_{V\,\rm nominal}^2 - \sigma_{V\rm test}^2|}}, \quad (2)$$

where V is the measured BF and σ_V is the statistical uncertainty of V. The ζ distribution is obtained by varying the fit range ten times, by shrinking or enlarging the interval (3390, 3590) MeV$/c^2$ to (3370, 3610) MeV$/c^2$, with a step of 2 MeV$/c^2$. After these tests, the associated systematic uncertainty is found to be negligible since the ζ distribution shows no significant deviation.

(c) *Signal shape*: To assess the systematic uncertainty due to the choice of signal shape, we use an alternative Breit-Wigner (BW) function $BW(M_{\Lambda\bar{\Lambda}\phi}) \times E_\gamma^3 \times D(E_\gamma)$ to describe the signal distribution, where $BW(M_{\Lambda\bar{\Lambda}\phi}) = ((M_{\Lambda\bar{\Lambda}\phi} - m_{\chi_{cJ}})^2 + \frac{1}{4}\Gamma_{\chi_{cJ}}^2)^{-1}$ [9] is the nonrelativistic BW function with width $\Gamma_{\chi_{cJ}}$ and mass $m_{\chi_{cJ}}$ fixed to their individual PDG values [1]; $E_\gamma = (m_{\psi(3686)}^2 - M_{\Lambda\bar{\Lambda}\phi}^2)/2m_{\psi(3686)}$ is the energy of the transition photon in the $\psi(3686)$ rest frame; and $D(E_\gamma)$ is a damping factor that suppresses the divergent tail due to E_γ^3. This damping factor is described by $D(E_\gamma) = \exp(-E_\gamma^2/8\beta^2)$ with β constrained to the CLEO measurement (65.0 ± 2.5) MeV [34]. The difference in the signal yields between fits with the two different signal functions is taken as the systematic uncertainty.

(d) *Background shape*: The systematic uncertainties due to the background shape are estimated by replacing the MC-simulated shape of $\psi(3686) \to \gamma\Lambda\bar{\Lambda}\phi$ with a second-order polynomial function. The change of the fitted signal yield is taken as the systematic uncertainty.

(e) *Normalization factor*: The systematic uncertainty of the normalization factor of the ϕ sideband, f_ϕ, is estimated by varying the sideband region by $\pm 1\sigma$, where σ denotes the mass

TABLE II. Systematic uncertainties (%) in the BF measurements, where "neg" indicates that the associated systematic uncertainty is negligible, and the three dots indicates that the systematic uncertainty is not applicable.

Source	χ_{c0}	χ_{c1}	χ_{c2}
Kaon tracking	2.0	2.0	2.0
Kaon PID	2.0	2.0	2.0
Photon reconstruction	1.0	1.0	1.0
4C kinematic fit	1.3	1.3	1.3
Λ reconstruction	1.8	1.8	1.8
$\bar{\Lambda}$ reconstruction	1.5	1.5	1.5
Mass window	1.0	0.4	1.0
Fit range	neg	neg	neg
Signal shape	3.1	3.1	0.5
Background shape	2.8	0.8	0.3
Normalization factor	0.3	0.2	0.3
MC model	$\cdots$	2.6	0.5
Input BFs	2.8	3.1	2.8
$N_{\psi(3686)}$	0.5	0.5	0.5
Total	6.5	6.6	5.1

resolution. The largest differences of the BFs from the baseline results are assigned as the corresponding systematic uncertainties.

(7) *MC model*: The systematic uncertainty due to the MC model is estimated by varying the bin size by $\pm 25\%$, and varying the number of background events by 1 standard deviation in the input Dalitz plot in the BODY3 generator, under the assumption that the background satisfies a Poisson distribution. Combining the results from the two sources, the larger difference relative to the baseline efficiency is used to determine the systematic uncertainty.

(8) *Input BFs*: The uncertainties of the BFs of $\psi(3686) \to \gamma\chi_{c0}$, $\psi(3686) \to \gamma\chi_{c1}$, $\psi(3686) \to \gamma\chi_{c2}$, $\Lambda \to p\pi$, and $\phi \to K^+K^-$ taken from the PDG [1] are 2.0%, 2.5%, 2.1%, 1.6% and 1.0%, respectively.

(9) $N_{\psi(3686)}$: The uncertainty on the value of the total number of $\psi(3686)$ events, determined with inclusive hadronic $\psi(3686)$ decays, is 0.5% [11].

All the systematic uncertainties are assumed to be independent of each other and combined in quadrature to obtain the overall systematic uncertainty as listed in Table II.

VII. SUMMARY

By analyzing $(2712.4 \pm 14.3) \times 10^6$ $\psi(3686)$ events, we observe the signals of $\chi_{c1,2} \to \Lambda\bar{\Lambda}\phi$ for the first time and find the evidence of $\chi_{c0} \to \Lambda\bar{\Lambda}\phi$ with a significance of 4.1σ. We determine their decay BFs to be $\mathcal{B}(\chi_{c0} \to \Lambda\bar{\Lambda}\phi) = (2.99 \pm 1.24 \pm 0.19) \times 10^{-5}$, $\mathcal{B}(\chi_{c1} \to \Lambda\bar{\Lambda}\phi) = (6.01 \pm 0.90 \pm 0.40) \times 10^{-5}$ and $\mathcal{B}(\chi_{c2} \to \Lambda\bar{\Lambda}\phi) = (7.13 \pm 0.81 \pm 0.36) \times 10^{-5}$, where the first uncertainties are statistical and the second systematic. No obvious enhancement near the $\Lambda\bar{\Lambda}$ production threshold is found. No obvious excited Λ state is found in the $M_{\Lambda\phi}$ or $M_{\bar{\Lambda}\phi}$ spectra, either.

ACKNOWLEDGMENTS

The BESIII Collaboration thanks the staff of BEPCII and the IHEP computing center for their strong support. This work is supported in part by the National Key R&D Program of China under Contracts No. 2020YFA0406300 and No. 2020YFA0406400; National Natural Science Foundation of China (NSFC) under Contracts No. 11635010, No. 11735014, No. 11835012, No. 11935015, No. 11935016, No. 11935018, No. 11961141012, No. 12022510, No. 12025502, No. 12035009, No. 12035013, No. 12061131003, No. 12150004, No. 12192260, No. 12192261, No. 12192262, No. 12192263, No. 12192264, No. 12192265, No. 12221005, No. 12225509, No. 12235017, No. 12275058, and No. 12275067; Program of Science and Technology Development Plan of Jilin Province of China under Contracts No. 20210508047RQ and No. 20230101021JC; Natural Science Foundation of Henan Province (Grant No. 225200810030), and Excellent Youth Foundation of Henan Province (Grant No. 212300410010); the Chinese Academy of Sciences (CAS) Large-Scale Scientific Facility Program; the CAS Center for Excellence in Particle Physics (CCEPP); Joint Large-Scale Scientific Facility Funds of the NSFC and CAS under Contract No. U1832207; CAS Key Research Program of Frontier Sciences under Contracts No. QYZDJ-SSW-SLH003 and No. QYZDJ-SSW-SLH040; 100 Talents Program of CAS; The Institute of Nuclear and Particle Physics (INPAC) and Shanghai Key Laboratory for Particle Physics and Cosmology; European Union's Horizon 2020 research and innovation program under Marie Sklodowska-Curie Grant Agreement under Contract No. 894790; German Research Foundation DFG under Contract No. 455635585, Collaborative Research Center CRC No. 1044, No. FOR5327, and No. GRK 2149; Istituto Nazionale di Fisica Nucleare, Italy; Ministry of Development of Turkey under Contract No. DPT2006K-120470; National Research Foundation of Korea under Contract No. NRF-2022R1A2C1092335; National Science and Technology fund of Mongolia; National Science Research and Innovation Fund (NSRF) via the Program Management Unit for Human Resources & Institutional Development, Research and Innovation of Thailand under Contract No. B16F640076; Polish National Science Centre under Contract No. 2019/35/O/ST2/02907; The Swedish Research Council; and the U.S. Department of Energy under Contract No. DE-FG02-05ER41374.

[1] P. L. Workman *et al.* (Particle Data Group), Prog. Theor. Exp. Phys. **2022**, 083C01 (2022) and 2023 update.
[2] J. Z. Bai *et al.* (BES Collaboration), Phys. Rev. Lett. **91**, 022001 (2003).
[3] M. Ablikim *et al.* (BESIII Collaboration), Phys. Rev. Lett. **108**, 112003 (2012).
[4] M. Ablikim *et al.* (BESIII Collaboration), Phys. Rev. D **104**, 052006 (2021).
[5] L. Zhao, N. Li, S. L. Zhu, and B. S. Zou, Phys. Rev. D **87**, 054034 (2013).
[6] D. M. Manley *et al.* (Crystal Ball Collaboration), Phys. Rev. Lett. **88**, 012002 (2001).
[7] M. Ablikim *et al.* (BESIII Collaboration), Phys. Rev. D **106**, 072006 (2022).
[8] M. Ablikim *et al.* (BESIII Collaboration), Phys. Rev. D **87**, 012007 (2013).
[9] M. Ablikim *et al.* (BESIII Collaboration), J. High Energy Phys. 11 (2021) 217.
[10] M. Ablikim *et al.* (BESIII Collaboration), Phys. Rev. D **106**, 072004 (2022).
[11] M. Ablikim *et al.* (BESIII Collaboration), Chin. Phys. C **48**, 093001 (2024).
[12] M. Ablikim *et al.* (BESIII Collaboration), Nucl. Instrum. Methods Phys. Res., Sect. A **614**, 345 (2010).
[13] C. H. Yu *et al.*, *Proceedings of IPAC2016, Busan, Korea* (JACoW, Busan, 2016), https://accelconf.web.cern.ch/ipac2016/.
[14] X. Li *et al.*, Radiat. Detect. Tech. Methods **1**, 13 (2017).
[15] Y. X. Guo *et al.*, Radiat. Detect. Technol. Methods **1**, 15 (2017).
[16] P. Cao *et al.*, Nucl. Instrum. Methods Phys. Res., Sect. A **953**, 163053 (2020).
[17] S. Agostinelli *et al.* (GEANT4 Collaboration), Nucl. Instrum. Methods Phys. Res., Sect. A **506**, 250 (2003).
[18] K. X. Huang *et al.*, Nucl. Sci. Tech. **33**, 142 (2022).
[19] S. Jadach, B. F. L. Ward, and Z. Wąs, Comput. Phys. Commun. **130**, 260 (2000).
[20] S. Jadach, B. F. L. Ward, and Z. Wąs, Phys. Rev. D **63**, 113009 (2001).
[21] R. G. Ping, Chin. Phys. C **32**, 599 (2008).
[22] D. J. Lange, Nucl. Instrum. Methods Phys. Res., Sect. A **462**, 152 (2001).
[23] J. C. Chen, G. S. Huang, X. R. Qi, D. H. Zhang, and Y. S. Zhu, Phys. Rev. D **62**, 034003 (2000).
[24] R. L. Yang, R. G. Ping, and H. Chen, Chin. Phys. Lett. **31**, 061301 (2014).
[25] E. Richter-Wąs, Phys. Lett. B **303**, 163 (1993).
[26] M. Xu *et al.*, Chin. Phys. C **33**, 428 (2009).
[27] G. Punzi *et al.*, eConf C **030908**, MODT002 (2003), https://inspirehep.net/literature/634798.
[28] X. Y. Zhou, S. X. Du, G. Li, and C. P. Shen, Comput. Phys. Commun. **258**, 107540 (2021).
[29] H. Albrecht*et al.*, Phys. Lett. B **340**, 217 (1994).
[30] Y. S. Zhu, High Energy Phys. Nucl. Phys. **30**, 331 (2006), https://inspirehep.net/literature/805275.
[31] M. Ablikim *et al.* (BESIII Collaboration), Phys. Rev. D **83**, 112005 (2011).
[32] M. Ablikim *et al.* (BESIII Collaboration), Phys. Rev. D **81**, 052005 (2010).
[33] O. Behnke, K. Kröninger, G. Schott, and T. Schörner-Sadenius, *Data Analysis in High Energy Physics: A Practical Guide to Statistical Methods* (Wiley-VCH, Berlin, Germany, 2013).
[34] R. E. Mitchell *et al.* (CLEO Collaboration), Phys. Rev. Lett. **102**, 011801 (2009).

M. Ablikim,[1] M. N. Achasov,[4,c] P. Adlarson,[75] O. Afedulidis,[3] X. C. Ai,[80] R. Aliberti,[35] A. Amoroso,[74a,74c] Q. An,[71,58,a] Y. Bai,[57] O. Bakina,[36] I. Balossino,[29a] Y. Ban,[46,h] H.-R. Bao,[63] V. Batozskaya,[1,44] K. Begzsuren,[32] N. Berger,[35] M. Berlowski,[44] M. Bertani,[28a] D. Bettoni,[29a] F. Bianchi,[74a,74c] E. Bianco,[74a,74c] A. Bortone,[74a,74c] I. Boyko,[36] R. A. Briere,[5] A. Brueggemann,[68] H. Cai,[76] X. Cai,[1,58] A. Calcaterra,[28a] G. F. Cao,[1,63] N. Cao,[1,63] S. A. Cetin,[62a] J. F. Chang,[1,58] G. R. Che,[43] G. Chelkov,[36,b] C. Chen,[43] C. H. Chen,[9] Chao Chen,[55] G. Chen,[1] H. S. Chen,[1,63] H. Y. Chen,[20] M. L. Chen,[1,58,63] S. J. Chen,[42] S. L. Chen,[45] S. M. Chen,[61] T. Chen,[1,63] X. R. Chen,[31,63] X. T. Chen,[1,63] Y. B. Chen,[1,58] Y. Q. Chen,[34] Z. J. Chen,[25,i] Z. Y. Chen,[1,63] S. K. Choi,[10] G. Cibinetto,[29a] F. Cossio,[74c] J. J. Cui,[50] H. L. Dai,[1,58] J. P. Dai,[78] A. Dbeyssi,[18] R. E. de Boer,[3] D. Dedovich,[36] C. Q. Deng,[72] Z. Y. Deng,[1] A. Denig,[35] I. Denysenko,[36] M. Destefanis,[74a,74c] F. De Mori,[74a,74c] B. Ding,[66,1] X. X. Ding,[46,h] Y. Ding,[34] Y. Ding,[40] J. Dong,[1,58] L. Y. Dong,[1,63] M. Y. Dong,[1,58,63] X. Dong,[76] M. C. Du,[1] S. X. Du,[80] Y. Y. Duan,[55] Z. H. Duan,[42] P. Egorov,[36,b] Y. H. Fan,[45] J. Fang,[1,58] J. Fang,[59] S. S. Fang,[1,63] W. X. Fang,[1] Y. Fang,[1] Y. Q. Fang,[1,58] R. Farinelli,[29a] L. Fava,[74b,74c] F. Feldbauer,[3] G. Felici,[28a] C. Q. Feng,[71,58] J. H. Feng,[59] Y. T. Feng,[71,58] M. Fritsch,[3] C. D. Fu,[1] J. L. Fu,[63] Y. W. Fu,[1,63] H. Gao,[63] X. B. Gao,[41] Y. N. Gao,[46,h] Yang Gao,[71,58] S. Garbolino,[74c] I. Garzia,[29a,29b] L. Ge,[80] P. T. Ge,[76] Z. W. Ge,[42] C. Geng,[59] E. M. Gersabeck,[67] A. Gilman,[69] K. Goetzen,[13] L. Gong,[40] W. X. Gong,[1,58] W. Gradl,[35] S. Gramigna,[29a,29b] M. Greco,[74a,74c] M. H. Gu,[1,58] Y. T. Gu,[15] C. Y. Guan,[1,63] A. Q. Guo,[31,63] L. B. Guo,[41] M. J. Guo,[50] R. P. Guo,[49] Y. P. Guo,[12,g] A. Guskov,[36,b] J. Gutierrez,[27] K. L. Han,[63] T. T. Han,[1] F. Hanisch,[3] X. Q. Hao,[19] F. A. Harris,[65] K. K. He,[55] K. L. He,[1,63] F. H. Heinsius,[3] C. H. Heinz,[35] Y. K. Heng,[1,58,63] C. Herold,[60] T. Holtmann,[3] P. C. Hong,[34] G. Y. Hou,[1,63] X. T. Hou,[1,63] Y. R. Hou,[63] Z. L. Hou,[1] B. Y. Hu,[59] H. M. Hu,[1,63] J. F. Hu,[56,j] S. L. Hu,[12,g] T. Hu,[1,58,63] Y. Hu,[1] G. S. Huang,[71,58] K. X. Huang,[59] L. Q. Huang,[31,63] X. T. Huang,[50] Y. P. Huang,[1] Y. S. Huang,[59] T. Hussain,[73] F. Hölzken,[3] N. Hüsken,[35] N. in der Wiesche,[68] J. Jackson,[27] S. Janchiv,[32] J. H. Jeong,[10] Q. Ji,[1] Q. P. Ji,[19] W. Ji,[1,63] X. B. Ji,[1,63] X. L. Ji,[1,58] Y. Y. Ji,[50] X. Q. Jia,[50] Z. K. Jia,[71,58] D. Jiang,[1,63] H. B. Jiang,[76] P. C. Jiang,[46,h]

S. S. Jiang,[39] T. J. Jiang,[16] X. S. Jiang,[1,58,63] Y. Jiang,[63] J. B. Jiao,[50] J. K. Jiao,[34] Z. Jiao,[23] S. Jin,[42] Y. Jin,[66] M. Q. Jing,[1,63] X. M. Jing,[63] T. Johansson,[75] S. Kabana,[33] N. Kalantar-Nayestanaki,[64] X. L. Kang,[9] X. S. Kang,[40] M. Kavatsyuk,[64] B. C. Ke,[80] V. Khachatryan,[27] A. Khoukaz,[68] R. Kiuchi,[1] O. B. Kolcu,[62a] B. Kopf,[3] M. Kuessner,[3] X. Kui,[1,63] N. Kumar,[26] A. Kupsc,[44,75] W. Kühn,[37] J. J. Lane,[67] P. Larin,[18] L. Lavezzi,[74a,74c] T. T. Lei,[71,58] Z. H. Lei,[71,58] M. Lellmann,[35] T. Lenz,[35] C. Li,[47] C. Li,[43] C. H. Li,[39] Cheng Li,[71,58] D. M. Li,[80] F. Li,[1,58] G. Li,[1] H. B. Li,[1,63] H. J. Li,[19] H. N. Li,[56,j] Hui Li,[43] J. R. Li,[61] J. S. Li,[59] K. Li,[1] L. J. Li,[1,63] L. K. Li,[1] Lei Li,[48] M. H. Li,[43] P. R. Li,[38,k,l] Q. M. Li,[1,63] Q. X. Li,[50] R. Li,[17,31] S. X. Li,[12] T. Li,[50] W. D. Li,[1,63] W. G. Li,[1,a] X. Li,[1,63] X. H. Li,[71,58] X. L. Li,[50] X. Y. Li,[1,63] X. Z. Li,[59] Y. G. Li,[46,h] Z. J. Li,[59] Z. Y. Li,[78] C. Liang,[42] H. Liang,[1,63] H. Liang,[71,58] Y. F. Liang,[54] Y. T. Liang,[31,63] G. R. Liao,[14] L. Z. Liao,[50] Y. P. Liao,[1,63] J. Libby,[26] A. Limphirat,[60] C. C. Lin,[55] D. X. Lin,[31,63] T. Lin,[1] B. J. Liu,[1] B. X. Liu,[76] C. Liu,[34] C. X. Liu,[1] F. Liu,[1] F. H. Liu,[53] Feng Liu,[6] G. M. Liu,[56,j] H. Liu,[38,k,l] H. B. Liu,[15] H. H. Liu,[1] H. M. Liu,[1,63] Huihui Liu,[21] J. B. Liu,[71,58] J. Y. Liu,[1,63] K. Liu,[38,k,l] K. Y. Liu,[40] Ke Liu,[22] L. Liu,[71,58] L. C. Liu,[43] Lu Liu,[43] M. H. Liu,[12,g] P. L. Liu,[1] Q. Liu,[63] S. B. Liu,[71,58] T. Liu,[12,g] W. K. Liu,[43] W. M. Liu,[71,58] X. Liu,[38,k,l] X. Liu,[39] Y. Liu,[80] Y. Liu,[38,k,l] Y. B. Liu,[43] Z. A. Liu,[1,58,63] Z. D. Liu,[9] Z. Q. Liu,[50] X. C. Lou,[1,58,63] F. X. Lu,[59] H. J. Lu,[23] J. G. Lu,[1,58] X. L. Lu,[1] Y. Lu,[7] Y. P. Lu,[1,58] Z. H. Lu,[1,63] C. L. Luo,[41] J. R. Luo,[59] M. X. Luo,[79] T. Luo,[12,g] X. L. Luo,[1,58] X. R. Lyu,[63] Y. F. Lyu,[43] F. C. Ma,[40] H. Ma,[78] H. L. Ma,[1] J. L. Ma,[1,63] L. L. Ma,[50] M. M. Ma,[1,63] Q. M. Ma,[1] R. Q. Ma,[1,63] T. Ma,[71,58] X. T. Ma,[1,63] X. Y. Ma,[1,58] Y. Ma,[46,h] Y. M. Ma,[31] F. E. Maas,[18] M. Maggiora,[74a,74c] S. Malde,[69] Y. J. Mao,[46,h] Z. P. Mao,[1] S. Marcello,[74a,74c] Z. X. Meng,[66] J. G. Messchendorp,[13,64] G. Mezzadri,[29a] H. Miao,[1,63] T. J. Min,[42] R. E. Mitchell,[27] X. H. Mo,[1,58,63] B. Moses,[27] N. Yu. Muchnoi,[4,c] J. Muskalla,[35] Y. Nefedov,[36] F. Nerling,[18,e] L. S. Nie,[20] I. B. Nikolaev,[4,c] Z. Ning,[1,58] S. Nisar,[11,m] Q. L. Niu,[38,k,l] W. D. Niu,[55] Y. Niu,[50] S. L. Olsen,[63] Q. Ouyang,[1,58,63] S. Pacetti,[28b,28c] X. Pan,[55] Y. Pan,[57] A. Pathak,[34] P. Patteri,[28a] Y. P. Pei,[71,58] M. Pelizaeus,[3] H. P. Peng,[71,58] Y. Y. Peng,[38,k,l] K. Peters,[13,e] J. L. Ping,[41] R. G. Ping,[1,63] S. Plura,[35] V. Prasad,[33] F. Z. Qi,[1] H. Qi,[71,58] H. R. Qi,[61] M. Qi,[42] T. Y. Qi,[12,g] S. Qian,[1,58] W. B. Qian,[63] C. F. Qiao,[63] X. K. Qiao,[80] J. J. Qin,[72] L. Q. Qin,[14] L. Y. Qin,[71,58] X. S. Qin,[50] Z. H. Qin,[1,58] J. F. Qiu,[1] Z. H. Qu,[72] C. F. Redmer,[35] K. J. Ren,[39] A. Rivetti,[74c] M. Rolo,[74c] G. Rong,[1,63] Ch. Rosner,[18] S. N. Ruan,[43] N. Salone,[44] A. Sarantsev,[36,d] Y. Schelhaas,[35] K. Schoenning,[75] M. Scodeggio,[29a] K. Y. Shan,[12,g] W. Shan,[24] X. Y. Shan,[71,58] Z. J. Shang,[38,k,l] L. G. Shao,[1,63] M. Shao,[71,58] C. P. Shen,[12,g] H. F. Shen,[1,8] W. H. Shen,[63] X. Y. Shen,[1,63] Y. M. Shen,[19] B. A. Shi,[63] H. Shi,[71,58] H. C. Shi,[71,58] J. L. Shi,[12,g] J. Y. Shi,[1] Q. Q. Shi,[55] S. Y. Shi,[72] X. Shi,[1,58] J. J. Song,[19] T. Z. Song,[59] W. M. Song,[34,1] Y. J. Song,[12,g] Y. X. Song,[46,h,n] S. Sosio,[74a,74c] S. Spataro,[74a,74c] F. Stieler,[35] Y. J. Su,[63] G. B. Sun,[76] G. X. Sun,[1] H. Sun,[63] H. K. Sun,[1] J. F. Sun,[19] K. Sun,[61] L. Sun,[76] S. S. Sun,[1,63] T. Sun,[51,f] W. Y. Sun,[34] Y. Sun,[9] Y. J. Sun,[71,58] Y. Z. Sun,[1] Z. Q. Sun,[1,63] Z. T. Sun,[50] C. J. Tang,[54] G. Y. Tang,[1] J. Tang,[59] M. Tang,[71,58] Y. A. Tang,[76] L. Y. Tao,[72] Q. T. Tao,[25,i] M. Tat,[69] J. X. Teng,[71,58] V. Thoren,[75] W. H. Tian,[59] Y. Tian,[31,63] Z. F. Tian,[76] I. Uman,[62b] Y. Wan,[55] S. J. Wang,[50] B. Wang,[1] B. L. Wang,[63] Bo Wang,[71,58] D. Y. Wang,[46,h] F. Wang,[72] H. J. Wang,[38,k,l] J. J. Wang,[76] J. P. Wang,[50] K. Wang,[1,58] L. L. Wang,[1] M. Wang,[50] N. Y. Wang,[63] S. Wang,[38,k,l] S. Wang,[12,g] T. Wang,[12,g] T. J. Wang,[43] W. Wang,[59] W. Wang,[72] W. P. Wang,[35,71,o] X. Wang,[46,h] X. F. Wang,[38,k,l] X. J. Wang,[39] X. L. Wang,[12,g] X. N. Wang,[1] Y. Wang,[61] Y. D. Wang,[45] Y. F. Wang,[1,58,63] Y. L. Wang,[19] Y. N. Wang,[45] Y. Q. Wang,[1] Yaqian Wang,[17] Yi Wang,[61] Z. Wang,[1,58] Z. L. Wang,[72] Z. Y. Wang,[1,63] Ziyi Wang,[63] D. H. Wei,[14] F. Weidner,[68] S. P. Wen,[1] Y. R. Wen,[39] U. Wiedner,[3] G. Wilkinson,[69] M. Wolke,[75] L. Wollenberg,[3] C. Wu,[39] J. F. Wu,[1,8] L. H. Wu,[1] L. J. Wu,[1,63] X. Wu,[12,g] X. H. Wu,[34] Y. Wu,[71,58] Y. H. Wu,[55] Y. J. Wu,[31] Z. Wu,[1,58] L. Xia,[71,58] X. M. Xian,[39] B. H. Xiang,[1,63] T. Xiang,[46,h] D. Xiao,[38,k,l] G. Y. Xiao,[42] S. Y. Xiao,[1] Y. L. Xiao,[12,g] Z. J. Xiao,[41] C. Xie,[42] X. H. Xie,[46,h] Y. Xie,[50] Y. G. Xie,[1,58] Y. H. Xie,[6] Z. P. Xie,[71,58] T. Y. Xing,[1,63] C. F. Xu,[1,63] C. J. Xu,[59] G. F. Xu,[1] H. Y. Xu,[66,2,p] M. Xu,[71,58] Q. J. Xu,[16] Q. N. Xu,[30] W. Xu,[1] W. L. Xu,[66] X. P. Xu,[55] Y. C. Xu,[77] Z. P. Xu,[42] Z. S. Xu,[63] F. Yan,[12,g] L. Yan,[12,g] W. B. Yan,[71,58] W. C. Yan,[80] X. Q. Yan,[1] H. J. Yang,[51,f] H. L. Yang,[34] H. X. Yang,[1] T. Yang,[1] Y. Yang,[12,g] Y. F. Yang,[1,63] Y. F. Yang,[43] Y. X. Yang,[1,63] Z. W. Yang,[38,k,l] Z. P. Yao,[50] M. Ye,[1,58] M. H. Ye,[8] J. H. Yin,[1] Z. Y. You,[59] B. X. Yu,[1,58,63] C. X. Yu,[43] G. Yu,[1,63] J. S. Yu,[25,i] T. Yu,[72] X. D. Yu,[46,h] Y. C. Yu,[80] C. Z. Yuan,[1,63] J. Yuan,[34] J. Yuan,[45] L. Yuan,[2] S. C. Yuan,[1,63] Y. Yuan,[1,63] Z. Y. Yuan,[59] C. X. Yue,[39] A. A. Zafar,[73] F. R. Zeng,[50] S. H. Zeng,[72] X. Zeng,[12,g] Y. Zeng,[25,i] Y. J. Zeng,[59] Y. J. Zeng,[1,63] X. Y. Zhai,[34] Y. C. Zhai,[50] Y. H. Zhan,[59] A. Q. Zhang,[1,63] B. L. Zhang,[1,63] B. X. Zhang,[1] D. H. Zhang,[43] G. Y. Zhang,[19] H. Zhang,[71,58] H. Zhang,[80] H. C. Zhang,[1,58,63] H. H. Zhang,[34] H. H. Zhang,[59] H. Q. Zhang,[1,58,63] H. R. Zhang,[71,58] H. Y. Zhang,[1,58] J. Zhang,[80] J. Zhang,[59] J. J. Zhang,[52] J. L. Zhang,[20] J. Q. Zhang,[41] J. S. Zhang,[12,g] J. W. Zhang,[1,58,63] J. X. Zhang,[38,k,l] J. Y. Zhang,[1] J. Z. Zhang,[1,63] Jianyu Zhang,[63] L. M. Zhang,[61] Lei Zhang,[42] P. Zhang,[1,63] Q. Y. Zhang,[34] R. Y. Zhang,[38,k,l] S. H. Zhang,[1,63] Shulei Zhang,[25,i] X. D. Zhang,[45] X. M. Zhang,[1] X. Y. Zhang,[50] Y. Zhang,[72] Y. Zhang,[1] Y. T. Zhang,[80] Y. H. Zhang,[1,58] Y. M. Zhang,[39] Yan Zhang,[71,58] Z. D. Zhang,[1] Z. H. Zhang,[1] Z. L. Zhang,[34]

Z. Y. Zhang,[76] Z. Y. Zhang,[43] Z. Z. Zhang,[45] G. Zhao,[1] J. Y. Zhao,[1,63] J. Z. Zhao,[1,58] L. Zhao,[1] Lei Zhao,[71,58] M. G. Zhao,[43] N. Zhao,[78] R. P. Zhao,[63] S. J. Zhao,[80] Y. B. Zhao,[1,58] Y. X. Zhao,[31,63] Z. G. Zhao,[71,58] A. Zhemchugov,[36,b] B. Zheng,[72] B. M. Zheng,[34] J. P. Zheng,[1,58] W. J. Zheng,[1,63] Y. H. Zheng,[63] B. Zhong,[41] X. Zhong,[59] H. Zhou,[50] J. Y. Zhou,[34] L. P. Zhou,[1,63] S. Zhou,[6] X. Zhou,[76] X. K. Zhou,[6] X. R. Zhou,[71,58] X. Y. Zhou,[39] Y. Z. Zhou,[12,g] J. Zhu,[43] K. Zhu,[1] K. J. Zhu,[1,58,63] K. S. Zhu,[12,g] L. Zhu,[34] L. X. Zhu,[63] S. H. Zhu,[70] S. Q. Zhu,[42] T. J. Zhu,[12,g] W. D. Zhu,[41] Y. C. Zhu,[71,58] Z. A. Zhu,[1,63] J. H. Zou,[1] and J. Zu[71,58]

(BESIII Collaboration)

[1]*Institute of High Energy Physics, Beijing 100049, People's Republic of China*
[2]*Beihang University, Beijing 100191, People's Republic of China*
[3]*Bochum Ruhr-University, D-44780 Bochum, Germany*
[4]*Budker Institute of Nuclear Physics SB RAS (BINP), Novosibirsk 630090, Russia*
[5]*Carnegie Mellon University, Pittsburgh, Pennsylvania 15213, USA*
[6]*Central China Normal University, Wuhan 430079, People's Republic of China*
[7]*Central South University, Changsha 410083, People's Republic of China*
[8]*China Center of Advanced Science and Technology, Beijing 100190, People's Republic of China*
[9]*China University of Geosciences, Wuhan 430074, People's Republic of China*
[10]*Chung-Ang University, Seoul 06974, Republic of Korea*
[11]*COMSATS University Islamabad, Lahore Campus, Defence Road, Off Raiwind Road, 54000 Lahore, Pakistan*
[12]*Fudan University, Shanghai 200433, People's Republic of China*
[13]*GSI Helmholtzcentre for Heavy Ion Research GmbH, D-64291 Darmstadt, Germany*
[14]*Guangxi Normal University, Guilin 541004, People's Republic of China*
[15]*Guangxi University, Nanning 530004, People's Republic of China*
[16]*Hangzhou Normal University, Hangzhou 310036, People's Republic of China*
[17]*Hebei University, Baoding 071002, People's Republic of China*
[18]*Helmholtz Institute Mainz, Staudinger Weg 18, D-55099 Mainz, Germany*
[19]*Henan Normal University, Xinxiang 453007, People's Republic of China*
[20]*Henan University, Kaifeng 475004, People's Republic of China*
[21]*Henan University of Science and Technology, Luoyang 471003, People's Republic of China*
[22]*Henan University of Technology, Zhengzhou 450001, People's Republic of China*
[23]*Huangshan College, Huangshan 245000, People's Republic of China*
[24]*Hunan Normal University, Changsha 410081, People's Republic of China*
[25]*Hunan University, Changsha 410082, People's Republic of China*
[26]*Indian Institute of Technology Madras, Chennai 600036, India*
[27]*Indiana University, Bloomington, Indiana 47405, USA*
[28a]*INFN Laboratori Nazionali di Frascati, I-00044 Frascati, Italy*
[28b]*INFN Sezione di Perugia, I-06100 Perugia, Italy*
[28c]*University of Perugia, I-06100 Perugia, Italy*
[29a]*INFN Sezione di Ferrara, I-44122 Ferrara, Italy*
[29b]*University of Ferrara, I-44122 Ferrara, Italy*
[30]*Inner Mongolia University, Hohhot 010021, People's Republic of China*
[31]*Institute of Modern Physics, Lanzhou 730000, People's Republic of China*
[32]*Institute of Physics and Technology, Peace Avenue 54B, Ulaanbaatar 13330, Mongolia*
[33]*Instituto de Alta Investigación, Universidad de Tarapacá, Casilla 7D, Arica 1000000, Chile*
[34]*Jilin University, Changchun 130012, People's Republic of China*
[35]*Johannes Gutenberg University of Mainz, Johann-Joachim-Becher-Weg 45, D-55099 Mainz, Germany*
[36]*Joint Institute for Nuclear Research, 141980 Dubna, Moscow region, Russia*
[37]*Justus-Liebig-Universitaet Giessen, II. Physikalisches Institut, Heinrich-Buff-Ring 16, D-35392 Giessen, Germany*
[38]*Lanzhou University, Lanzhou 730000, People's Republic of China*
[39]*Liaoning Normal University, Dalian 116029, People's Republic of China*
[40]*Liaoning University, Shenyang 110036, People's Republic of China*
[41]*Nanjing Normal University, Nanjing 210023, People's Republic of China*
[42]*Nanjing University, Nanjing 210093, People's Republic of China*
[43]*Nankai University, Tianjin 300071, People's Republic of China*
[44]*National Centre for Nuclear Research, Warsaw 02-093, Poland*

[45]North China Electric Power University, Beijing 102206, People's Republic of China
[46]Peking University, Beijing 100871, People's Republic of China
[47]Qufu Normal University, Qufu 273165, People's Republic of China
[48]Renmin University of China, Beijing 100872, People's Republic of China
[49]Shandong Normal University, Jinan 250014, People's Republic of China
[50]Shandong University, Jinan 250100, People's Republic of China
[51]Shanghai Jiao Tong University, Shanghai 200240, People's Republic of China
[52]Shanxi Normal University, Linfen 041004, People's Republic of China
[53]Shanxi University, Taiyuan 030006, People's Republic of China
[54]Sichuan University, Chengdu 610064, People's Republic of China
[55]Soochow University, Suzhou 215006, People's Republic of China
[56]South China Normal University, Guangzhou 510006, People's Republic of China
[57]Southeast University, Nanjing 211100, People's Republic of China
[58]State Key Laboratory of Particle Detection and Electronics, Beijing 100049, Hefei 230026, People's Republic of China
[59]Sun Yat-Sen University, Guangzhou 510275, People's Republic of China
[60]Suranaree University of Technology, University Avenue 111, Nakhon Ratchasima 30000, Thailand
[61]Tsinghua University, Beijing 100084, People's Republic of China
[62a]Turkish Accelerator Center Particle Factory Group, Istinye University, 34010 Istanbul, Turkey
[62b]Near East University, Nicosia, North Cyprus, 99138, Mersin 10, Turkey
[63]University of Chinese Academy of Sciences, Beijing 100049, People's Republic of China
[64]University of Groningen, NL-9747 AA Groningen, The Netherlands
[65]University of Hawaii, Honolulu, Hawaii 96822, USA
[66]University of Jinan, Jinan 250022, People's Republic of China
[67]University of Manchester, Oxford Road, Manchester M13 9PL, United Kingdom
[68]University of Muenster, Wilhelm-Klemm-Strasse 9, 48149 Muenster, Germany
[69]University of Oxford, Keble Road, Oxford OX13RH, United Kingdom
[70]University of Science and Technology Liaoning, Anshan 114051, People's Republic of China
[71]University of Science and Technology of China, Hefei 230026, People's Republic of China
[72]University of South China, Hengyang 421001, People's Republic of China
[73]University of the Punjab, Lahore-54590, Pakistan
[74a]University of Turin and INFN, I-10125 Turin, Italy
[74b]University of Eastern Piedmont, I-15121 Alessandria, Italy
[74c]INFN, I-10125 Turin, Italy
[75]Uppsala University, Box 516, SE-75120 Uppsala, Sweden
[76]Wuhan University, Wuhan 430072, People's Republic of China
[77]Yantai University, Yantai 264005, People's Republic of China
[78]Yunnan University, Kunming 650500, People's Republic of China
[79]Zhejiang University, Hangzhou 310027, People's Republic of China
[80]Zhengzhou University, Zhengzhou 450001, People's Republic of China

[a]Deceased.
[b]Also at the Moscow Institute of Physics and Technology, Moscow 141700, Russia.
[c]Also at the Novosibirsk State University, Novosibirsk 630090, Russia.
[d]Also at the NRC "Kurchatov Institute," PNPI, 188300 Gatchina, Russia.
[e]Also at Goethe University Frankfurt, 60323 Frankfurt am Main, Germany.
[f]Also at Key Laboratory for Particle Physics, Astrophysics and Cosmology, Ministry of Education; Shanghai Key Laboratory for Particle Physics and Cosmology; Institute of Nuclear and Particle Physics, Shanghai 200240, People's Republic of China.
[g]Also at Key Laboratory of Nuclear Physics and Ion-Beam Application (MOE) and Institute of Modern Physics, Fudan University, Shanghai 200443, People's Republic of China.
[h]Also at State Key Laboratory of Nuclear Physics and Technology, Peking University, Beijing 100871, People's Republic of China.
[i]Also at School of Physics and Electronics, Hunan University, Changsha 410082, China.
[j]Also at Guangdong Provincial Key Laboratory of Nuclear Science, Institute of Quantum Matter, South China Normal University, Guangzhou 510006, China.
[k]Also at MOE Frontiers Science Center for Rare Isotopes, Lanzhou University, Lanzhou 730000, People's Republic of China.
[l]Also at Lanzhou Center for Theoretical Physics, Lanzhou University, Lanzhou 730000, People's Republic of China.
[m]Also at the Department of Mathematical Sciences, IBA, Karachi 75270, Pakistan.
[n]Also at Ecole Polytechnique Federale de Lausanne (EPFL), CH-1015 Lausanne, Switzerland.
[o]Also at Helmholtz Institute Mainz, Staudinger Weg 18, D-55099 Mainz, Germany.
[p]Also at School of Physics, Beihang University, Beijing 100191, China.